Minerals Engineering 134 (2019) 7–15

Contents lists available at ScienceDirect

Minerals Engineering

journal homepage: www.elsevier.com/locate/mineng

Modeling and energy-based model predictive control of high pressure grinding roll

Eduardo Vyhmeister[a,b,*], Lorenzo Reyes-Bozo[b], Roman Rodriguez-Maecker[c], Carlos Fúnez-Guerra[d], Fernando Cepeda-Vaca[c], Héctor Valdés-González[e]

[a] Insight Research Center, University Collage Cork, Cork, Ireland
[b] Universidad Central de Chile, Santiago, Chile
[c] Departamento de Energía y Mecánica, Universidad de las Fuerzas Armadas, ESPE, Extensión Latacunga, Latacunga, Ecuador
[d] Centro Nacional del Hidrógeno, Puertollano, Spain
[e] Facultad de Ingeniería, Universidad del Desarrollo, Santiago, Chile

ARTICLE INFO

Keywords:
High Pressure Grinding Roll (HPGR)
Modeling
Model predictive control

ABSTRACT

Even though semiautogenous grinding mills and ball mills are normally used in grinding processes, the industry is driven to decrease cost by increasing efficiencies and decreasing energy consumption. High Pressure Grinding Rolls (HPGR) are seen as an energy-efficient alternative but their developments in modeling and control have received relatively little attention. In this work a model and a control scheme for HPGR is presented that considers the total energy consumed as one of the main controlled variable. First, the model was generated by using literature-reported information of a specific manufacturer and lithology. The dynamic representation of the treatment capacity, product granulometric distribution (reported as 80% percentile), compression energy, and rolling energy were considered as the most important model output variables. Second, model validation was performed with considerable positive results (based on assessment of estimation errors). Finally, the model was used to generate a multiple input multiple output control scheme. As result, it was observed that the model had a correct representation of the phenomena involved and that the peripheral velocity and pressure used in the HPGR are useful manipulated variables to control the energy consumed by the equipment in an MPC scheme.

1. Introduction

Among the different processes involved in the mineral industry, comminution is known for being energy intensive (Salazar et al., 2014). In the USA, grinding processes account for approximately 29.3% of mining energy consumption (Tromans, 2008); globally, magnitudes in the order of 4% of electrical energy are reported (Jeswiet and Szekeres, 2016). Given this scenario, considerable part of the operational costs of concentrator plants are related to energy (in the order of 50%–70%; Salazar et al., 2014; Jeswiet and Szekeres, 2016). The industry is driven to decrease cost by increasing efficiencies and decreasing energy consumption. As shown by Schönert (Schönert, 1985, 1988), particle compression between surfaces is more energetically efficient than other grinding methods (in the order of 3 kWh/ton). Based on these fundamental studies the High Pressure Grinding Roll (HPGR) operational unit was designed. Considering its efficiency and its positive results in the cement industry, the HPGR has been seen as a viable alternative in the mining industries (Barrios and Tavares, 2016). In addition to its energy efficiency, the HPGR has improved effects on downstream operational units given by micro-fragmentation and dry/wet feed handling capabilities (up to about 10% of water) (Palm et al., 2010; Chapman et al., 2013; Barani and Balochi, 2016a; Morley, 2006). One of the drawbacks of the HPGR unit is that, as shown by Fuerstenau et al. (1996), grinding can come to a halt under specific operational conditions (high operational pressure).

The HPGR is basically a pair of counter rotating rolls mounted in a frame. A chute placed over the rolls is used to distribute the feed. By the use of a hydraulic system, one of the rolls supplies the necessary force to produce the particle compression. The feeding particles, which are forced to move across an opening given by the distance between the rolls, are semiautogenously grinded by an interparticle breakage mechanism (Barrios and Tavares, 2016). HPGR can be placed in comminution layouts as an open or closed circuit. Studies have been performed in order to evaluate the most efficient layout in the cement industry and general ores (Altun et al., 2011, Rosario, 2017). As pointed out in the work of Rosario (2017), the HPGR has considered to be used, as standard, as a tertiary crusher, in closed-circuit, with wet fine

* Corresponding author.
E-mail address: eduardo.vyhmeister@gmail.com (E. Vyhmeister).

https://doi.org/10.1016/j.mineng.2019.01.016
Received 28 January 2018; Received in revised form 29 October 2018; Accepted 10 January 2019
Available online 23 January 2019
0892-6875/

Nomenclature

Xc	critical size, m
D	roll diameter, m
O	gap, m
Z	height from the extrusion zone, m
L	depth of the HPGR unit, m
A	transversal area, m^2
V	volume, m^3
$\vec{v}$	material stripe velocity, m/s
U	rolls peripheral velocity, m/s
f	feed, kg/s
G_s	treatment capacity, kg/s
F	formation of particle of specific size, kg/s
D	destruction of particle of specific size, kg/s
M	total mass, kg
H	hold up mass in the block, kg
w	total mass for a specific size, kg
ρ	density, kg/m^3
ξ	corrected specific energy, kWh/kg
E, Ec, E'	specific energy (general, by compression, total), kWh/kg
P	power, kW
Pr	rotational power, kW
Rp	pressure, kg/m·s
F	compressive force, $kg{\cdot}m/s^2$
τ	torque, $kg{\cdot}m^2/s^2$
α	angle from the HPGR extrusion zone degrees
x	size-class –
S	specific breakage rate –
b	breakage distribution –
ω	mass fraction –

Parameters

B, β_1, β_2, β_3	breakage distribution parameter
τ	dissipated energy
ζ_1, ζ_2	breakage rate parameters
k_0	pre-exponential kinetic parameter
$\Delta E_{k,l}$	specific energy requirement to rupture a particle of size l and composition k

Subindexes

f	feed section
n	bottom section
cm	center of mass
i	section of the HPGR units (considering horizontal subdivisions)
j	particle size type j
l	particle size type l
k	composition of the k-type (considered homogeneous in this work)
ip	interparticle compression
sp	isolated compression/acceleration/de-aeration/pre-crushing/pre-grinding zone
a	apparent (for density)
s	solid (for density)

MPC-Variables

Λ, Γ	weight parameters
S	set point
M, P	manipulated (M) and predictive (P) horizon
y, u	controlled (y) and manipulated (u) variables

screens. Nevertheless, his work and others (Altun et al., 2011; Jankovic et al., 2013) have shown that there is still space for research and improvements regarding industrial layouts and circuit operations, especially if the information of the ore under consideration has not been fully evaluated. Independent of the previous statement, is expected that recycling material could result in finer product size distribution, since recycling material would occupy voids, improving the transfer of energy by the HPGR unit (Altun et al., 2011).

Even when the industry is currently focused on developing new applications for HPGR, accurate models for prediction, scale-up, and control are required in order to improve the HPGR units design and operations. Most of the current representations of HPGR units are based on steady-state models which are adequate for plant design and/or offline optimization, nevertheless they are wholly inadequate for process control or online optimization. As pointed out in the review by Rashidi et al. (2017), the development of realistic mathematical models for HPGR reduction size has not been possible due to its quick incorporation in the industry, among other reasons. Different models have been developed for HPGR representations however, the non-time dependent representations, complexity, and/or numerical solution (such as in discrete element methods; Barrios and Tavares (2016)) can have negative effects on its application (such as impossibility to be used in time-based controllers and considerable computational time). Furthermore, modeling publications tend to be limited and scattered (Rashidi et al., 2017). Overall, HPGR modeling has not yet been consolidated over every operational condition (type of ore, hardness, operational gap, among other conditions; e.g. Daniel and Morrel throughput model can fail over some specific conditions, Daniel and Morrel, 2004), so research dedicated to this field should be welcomed. Independent of the energy consumption reduction in HPGR and a design of ideal circuits for a given requirement, process control offers a recognized potential to achieve lower costs (lower energy consumption), higher yields, and/or higher stability in the product. In order to be successful, the process control requires a valid dynamic representation of the system therefore, the dilemma of finding a suitable representation of the system emerges again.

Historically, Proportional-Integral-Derivative (PID) control strategies have dominated industrial applications due to their design simplicity and performance for simple systems (Cao and Cao, 2006). Given an increasing necessity of controlling multivariable or complex systems, which can possess inverse dynamics or considerable time delay responses (common in mining operations but not necessarily in HPGR units), advanced control strategies have been considered. In the comminution processes, control strategies such as Model Predictive Control (Ramasamy et al., 2005), Neuro-control (Conradie and Aldrich, 2001), and Expert Control (Bouché et al., 2005), among others, have been implemented to varying degrees of success. The Model Predictive Control (MPC) is an optimization-based control accepted for its simple tuning process, applicability to Multiple Input Multiple Output (MIMO) systems, and handling of constraints (such as maximum allowed pressure for the current system). The combination of the MPC characteristics could be an ideal combination for controlling HPGR units. Nevertheless, a dynamic model that takes into account the complexity of grinding kinetics involved in a system of variable control volume with fast dynamics is essential. As observed in literature, the works focused on HPGR control are few (as far as author noticed unexistence for MPC), possible by their fast industrialization, lack of data, measuring of on-line variables, and fast dynamics, among other reasons that could change in time.

Based on the previous information, this work focuses on HPGR dynamic modeling. Step-response representations are obtained and used to construct a MIMO MPC. The MPC considered the total energy consumed by the equipment and the product particle size-distribution as the main controlled variables. The model is based in the works of Torres and Cassali (2009) and results are compared with the same

experimental information. Major modifications are performed in the modeling once compared with literature: the grinding kinetics are modified by using a typical chemical reaction first-order kinetic representation in which the selectivity of the reaction is estimated by a suitable breakage distribution. An Arrhenius-type kinetic parameter (in which the energy supplied would modify its value) is used to represent the energy effects. Generalization of the controller is made by considering that it operates in an open circuit (there is no specificity in the mining industry application). Recycling material would modify the feeds particle size distribution, and the model would not require any major modifications, other than parameters identification, in order to be used in closed circuit.

2. Modeling

The first step was the representation of the HPGR treatment capacity. To do that model, the idea of Austin's works (used by Torres and Cassali, 2009), in which two grinding zones are modeled by separate and interconnected, was used. The two zones are the isolated compression zone (SP-Zone, also known as the acceleration, de-aeration, pre-crushing or pre-grinding zone) and the interparticle compression zone (IP-Zone, also known as the grinding zone). In the first, the particles are gradually compacted and reoriented as they are forced to move in the direction of the rolls movement. Particles bigger than the space between the rolls (defined by a critical size, X_C) are grinded (given by the feed particle size-distribution and a breakage distribution; Whiten, 1973). In the second, the free space is almost inexistent, implying the most efficient use of the forces involved. The particles grinding phenomena can be represented in function of a specific breakage rate, a brakeage distribution, and a specific-sizes particles mass fraction (Torres and Cassali, 2009). The residence time of the solids through the IP-zone is a small fraction of the overall system; nevertheless, most of the phenomena involved are related to it (i.e. a thorough representation of this zone is essential).

Fig. 1 shows a schematic of a HPGR unit. The first and second zones are specified by angles (α_{IP} and α_{sP}, respectively). At the top of the figure, a chute has been vertically divided into two zones to clarify angles and distances used in the modeling process (left size) and create a representation of the phenomenon involved (right side). In here, D is the roll diameter; $G_{S,i}$ is the treatment capacity in the i^{th} section (delimited between the vertical heights Z_i and Z_{i+1}), α_i is the projected angle between the vertical heights Z_i and Z_{i+1}, and O_i is the gap at the lower height of the i-section (at the minimal distance between rolls, the gap is known as operational gap, O_n). The critical size can be calculated by Eq. (1) (Daniel and Morrell, 2004); here ρ_i is the apparent density (which considers the void fraction) in the i-position (feed, f or discharge, n). Other correlations can also be employed to estimate α_{sP} and therefore the critical size (Rashidi et al., 2017). Nevertheless, further information (gap porosity and throughput based on cake characteristic) are required.

$$X_C = \frac{1}{2}(D + O_n - \sqrt{(D + O_n)^2 - 4DO_n\rho_n/\rho_f}) \quad (1)$$

The treatment capacity in the SP-Zone was considered to be static, which means that the feed was equal to its discharge (assumption used for total mass but not for particle distribution). As specified by Torres and Cassali (2009), a center of mass expression is required in order to estimate the discharge flows in the IP-Zone. In the present work, the IP-Zone was horizontally subdivided in different blocks (ten in total). This division was performed to obtain a better representation of the dynamics involved in the most important phenomenological part of the HPGR. This subdivision implied different center of masses (one per each subdivision). The variation of the center of mass density (cm as sub index) in each block can be expressed as follows:

$$\frac{\partial\rho_{i,cm}}{\partial t} = \frac{G_{S,i-1} - G_{s,i}}{V_i} \quad (2)$$

The block volumes (V_i) are dependent on the number of subdivisions used, parameters (e.g. roll diameter), and dynamic variables (such as O_n and α_{IP}). For a given block, the treatment capacity can be estimated as described in Eq. (3), were $A_{\alpha_{i,cm}}$ is the transversal area located at the position of the i-block center of mass (Eq. (4)) and $\vec{v}_{i,cm}$ is the material stripe velocity (Eq. (5)). In these equations, L is the depth of the HPGR unit (perpendicular to the image shown in Fig. 1) and U is the rolls peripheral velocity.

$$G_{s,i} = \rho_{i,cm}A_{\alpha_{i,cm}}\vec{v}_{i,cm} \quad (3)$$

$$A_{\alpha_{i,cm}} = L(O_n + D(1 - cos(\alpha_{i,cm}))) \quad (4)$$

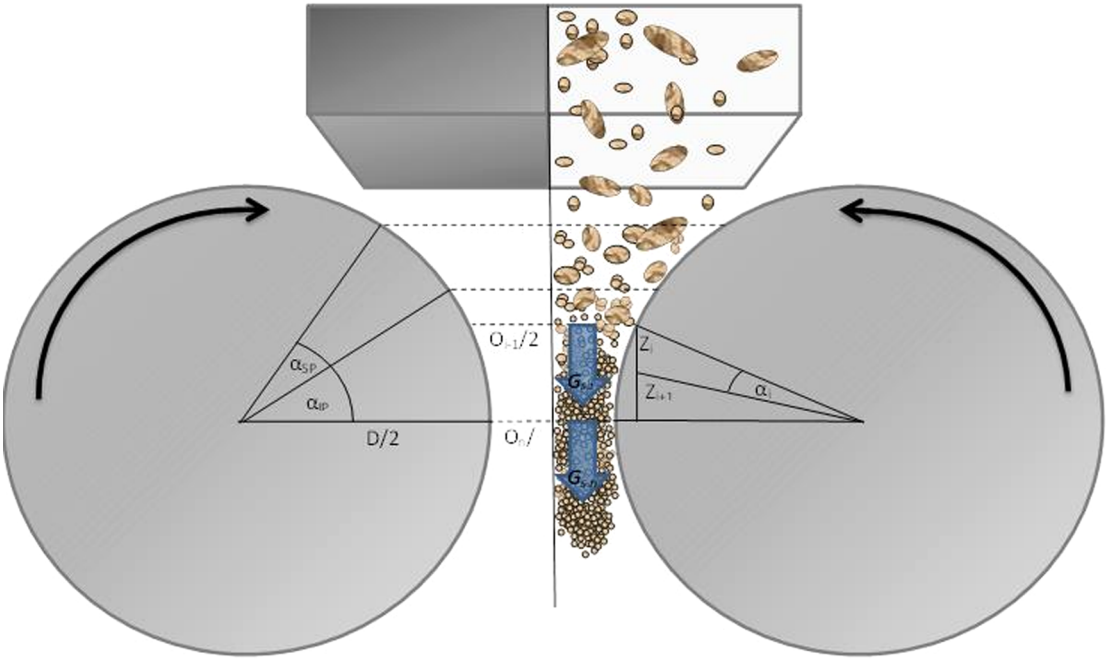

Fig. 1. HPGR schematic.

$$\vec{v}_{i,cm} = U\cos(\alpha_{i,cm}) \tag{5}$$

The volumes and angles involved in the calculation of each block were obtained by trigonometric considerations and the integration of the area involved. Eqs. (6) and (7) shows the integral of the area and its explicit evaluation (where Z is the altitude) while Eq. (8) shows the center of mass angle. Eq. (8) was obtained by considering that the density is reduced in function of the additional space that between rolls as the angle increases.

$$V_i = L\int_{Z_{i+1}}^{Z_i}\left(\frac{D}{2} + \frac{O_n}{2} - \sqrt{\left(\frac{D}{2}\right)^2 - z^2}\right)dz \tag{6}$$

$$V_i = L(D + O_n - 2\sqrt{(D/2)^2 - Z^2})Z - (\frac{D}{2})^2\left(asin\left(\frac{2Z}{D}\right) - \frac{sin\left(2asin(\frac{2Z}{D})\right)}{2}\right)\Bigg|_{Z_{i+1}}^{Z_i} \tag{7}$$

$$\alpha_{i,cm} = cos^{-1}\left(\frac{\rho_{i,cm}(O_n + D) - \rho_n O_n}{\rho_{i,cm} D}\right) \tag{8}$$

By solving previous equations, it is possible in each block to determinate both the dynamic variation of the density and the treatment capacity. It must be highlighted that the differential equation steady state was achieved (as evaluated in Matlab) when the angles were close to the inferior limit of each block. This result was obtained since the angle of the center of mass (Eq. (8)) is not completed disconnected from the previous equations. To avoid this, a dynamic integration of the density on each block could be considered, but this would imply an excessive use of computational times, making the modeling process too slow (as observed)). Alternatively, it can be considered that if the height of each block is relatively small (i.e. considerable subdivisions), the center of mass angle would be located relatively close to the center of each block. In the present work the latter assumption was employed. Although this approximation could introduce small errors, its consideration is an improvement to previous works in which the HPGR throughputs and holdups are evaluated by considering a constant behavior of the HPGR in the IP-zone (i.e. the same variables can be estimated only with the extrusion zone information).

For the product granulometric distribution the common representations used are first discussed. Then, the final model proposal used for dynamic control is presented.

The granulometric distribution at any point in the HPGR can be obtained by a dynamic balance of each particle considered in the system for the IP-Zone and by performing a rupture calculation of the particles bigger than the X_c for the SP-Zone. A total of 13 particle sizes ranges were considered in order to evaluate the model and compare the results with reported information (Torres and Cassali, 2009). The product granulometric distribution in the SP-Zone can be calculated by using the following expression (Whiten, 1973):

$$\omega_l = \sum_{j>Xc}^{N} b_{l,j,k} f_j \tag{9}$$

where $b_{l,j,k}$ is the brakeage distribution, which represents the percentage of the k-type composition particle of j-size that will be broken in a l-size particle; f_j represents the feed mass fraction of j-particle bigger than the critical size; and ω_l is the mass fraction of the l-size particle. In the present work a homogeneous composition was considered for simplicity and literature comparison. Therefore, the terms that are dependent on composition will be simplified (e.g. $b_{l,j,k}$ to $b_{l,j}$). The $b_{l,j}$, can be obtained by data back-calculations and from laboratory simulated experiments (Austin et al., 1984; Hinde and Kalala, 2009). Additionally, the $b_{l,j}$ can be obtained from the following equations, in which β_i are parameters that are functions of the material and type of equipment, while x_l is the l-particle size-class (Torres and Cassali, 2009).

$$b_{l,j} = B_{l-j+1} - B_{l-j+2} \quad If \quad l > j \tag{10}$$

$$b_{l,j} = 1 - \sum_j b_{i,j} \quad \Big| \quad If l = last \quad size \quad class \tag{11}$$

$$b_{l,j} = 0 \quad | \quad If \quad l < j \tag{12}$$

$$B_l = \beta_1\left(\frac{x_l}{x_2}\right)^{\beta_2} + (1 - \beta_1)\left(\frac{x_l}{x_2}\right)^{\beta_3} \tag{13}$$

The base equation normally used in the representation of tumbling or stirred media is given in Eq. (14) (Hinde and Kalala, 2009). Given that the IP-Zone was subdivided in ten blocks, a total of 130 differential equations dedicated to granulometric distribution were obtained. The number of Ordinary Differential Equations (ODEs) do not play a negative effect in the control process. The correlations used by the controller are between the manipulated/controlled variables (i.e. internal representations are not needed).

$$\frac{\partial H_i \cdot \omega_{j,i}}{\partial t} = G_{S,i-1}\omega_{j,i-1} - G_{S,i}P\omega_{j,i} + \sum_{s=1}^{m>j} F_s - D_j \tag{14}$$

In the previous equation, $\omega_{j,i}$ is the j-size particle mass fraction held in the i-block; H_i is the i-block total mass; F_s and D_j are the formation and destruction of particles. The total formation is a summation since contributions could come from any particles bigger than the j-particle. The pressure gradient in the HPGR width direction (parallel to O_n) can be used (an edge effect and the normal compression zone). The boundary between zones has been expressed in the work of Morrell et al. (1997). This gradient implies the vertical subdivisions of the blocks and therefore incorporation of several differential equations, leading to higher computational requirements. In the present work, these gradients were not considered and, as it will be seen in the results, the avoidance of this representation did not affect the model validation. Furthermore, the edge effect depends on the rolls housing (Rashidi et al., 2017), implying that it could be insignificant in some cases.

The formation and destruction of particles can be expressed in function of: a j-size class and k-type composition energy-normalized specific breakage rate (S_j^E), a brakeage distribution ($b_{l,j}$), and the mass of the j-size particle (w_j). S_j^E can be obtained from back-calculation or laboratory simulated experiments (Austin et al., 1984; Hinde and Kalala, 2009). In order to obtain a non-normalized energy specific breakage rate, the power (P) and total mass (M) have to be considered (Eqs. (15) and (16); Torres and Cassali, 2009).

$$S_j = \frac{P}{M}S_j^E \tag{15}$$

$$Ln\left(\frac{S_j^E}{S_1^E}\right) = \zeta_1 Ln\left(\frac{x_j}{x_1}\right) + \zeta_2 Ln\left(\frac{x_j}{x_1}\right)^2 \tag{16}$$

Eq. (14) can be simplified (and normally performed) if a perfectly mixed model (PMM) is assumed. This implies a perfect distribution (in any direction) and no holdups and, therefore, the first and second term of Eq. (14) are eliminated (Monov et al. 2012). Furthermore, as described by Fuerstenau et al. (1991) and stated in different works (Hinde and Kalala, 2009; Rashidi et al., 2017), the grinding kinetic in a HPGR is better represented by expressing the balance of each particle in function of the net specific energy input. This modification is achieved by considering that the increment in specific energy input is function of the specific power draft and time. By taking this consideration, the particle balance can be represented as:

$$\frac{\partial\omega_l(\xi)}{\partial\xi} = \sum_{j=1}^{l-1} S_j^E b_{l,j}\omega_j(\xi) - S_l^E\omega_l(\xi) \quad \text{with} \quad \xi = \frac{E^{1-\tau}}{1-\tau} \tag{17}$$

In this equation, E is the specific energy supplied [kWh/kg], $\omega_l(\xi)$ is the mass fraction in function of the specific energy input, and τ

($0 \leq \tau \leq 1$) is a parameter that represents the dissipated energy. As described by Fuerstenau et al. (1991), a set of first-order differential equations are formed which have an exponential-type solution of the different mass fractions. Even though the last expression can be used to estimate the product particle distributions, this representation is not useful in control processes. Some important considerations are:

- The time is not expressed as an independent variable. This implies that representation of the dynamics involved cannot be directly constructed (e.g. step-response, state-space). Similar consideration can be made to any model that only represent steady state scenarios.
- The variation of the feeds into the operational unit is not described, implying that variations on the products will only come from internal operational parameters (e.g. the specific energy supplied).
- The energy-normalized selection function (S_i^E) can be used for low specific energy input where there is a linear function between the energy input and the fineness of the product (Rashidi et al., 2017). Additionally, as explained in the work of Hinde and Kalala (2009), the relation between grind size and specific energy input is highly non-linear given by the reduction of the void volume, which results in a disproportional dissipation of energy.
- Even though the solutions of the differential equations have an exact solution, they cannot be used directly to generate time-dependent information.

Differently, Torres and Cassali (2009) derived a set of differential equations in which the variation of the mass fractions of an i-class size in function of a vertical distance was used. Similar to previous works, the PMM assumption was used. The lack of the time variable limits the applicability of the present model in control processes.

The consideration of no-variation in feed particle distribution can be assumed if the feed particle distribution is relatively constant, the range of a specific size-group is considerably large, and/or if the product particle distribution were not an important variable (which is not the case for a grinding process). For the cases in which the HPGR operates in a closed circuit, the feed will be formed from fresh and recycled material; this implies that both the feed and the recycled material will have to behave relatively constantly in order to consider them not important.

It should be pointed out that both previously referenced works (Torres and Cassali, 2009, and Fuerstenau et al., 1991) have avoided a direct dynamic representation of the HPGR units. This could be made for the HPGR and applied for specific control systems if the dynamics are considered almost instantaneous or not important. However, as can be observed in the literature, several of the models have been based on lab-scale information. As the systems are scaled up, circuits operate in a closed system, or the feeds behavior assumes values within wider ranges, the dynamic behaviors could assume an important factor in control and modelling.

Given the previous considerations, in the present work the expression given in Eq. (14) was modified and represented as a typical reaction model in which were incorporated a breakage distribution (which has intrinsically the same meaning as the selectivity), an Arrhenius-type kinetic parameter (in which the energy supplied would modify its value), and the particles compositions. Furthermore, the PMM was not considered in order to allow variations in the feed stream to have an effect in the system. The final representation used in this work is given in Eq. (18). Here the third term represents the formation of the particle of l-size that comes from the different contributions of particles bigger than l ($m > l$). The selectivity term defines what part of the particle will be grinded in a l-size ($b_{l,j}$). A first-order grinding kinetic with respect to the particle concentration was assumed (commonly assumed in grinding processes; Barani and Balochi, 2016b). The concentration is represented by the multiplication of the total mass in the i-block (H_i) and the particle mass fraction. Kinetic parameters represented by a pre-exponential term ($k_{0,l}$), which is specific to each l size particle, and an exponential term, which is calculated by a constant $\Delta E_{k,l}$, and the specific power consumption (E) were used. The parameter $\Delta E_{k,l}$ represents the specific energy required (in kWh/kg) to produce the rupture of the material of composition k and specific granulometric size l (similar to the activation energy).

$$\frac{\partial H_l \cdot \omega_{l,i}}{\partial t} = G_{S,i-1}\omega_{l,i-1} - G_{S,i}\omega_{l,i} + \sum_{s=1}^{m>l} H_i \cdot b_{l,s} \cdot \omega_{s,i} \cdot k_{0,s} e^{-\frac{\Delta E_{k,s}}{E}} - H_i \cdot \omega_{l,i} \cdot k_{0,l} \cdot e^{-\frac{\Delta E_{k,l}}{E}} \quad (18)$$

The HPGR models for power and specific energy consumed can be obtained from a set of equations that are based on Newtonian physics. The applied force (pressure) is split into two components, tangential and radial. The expressions of the power model are derived from a free-body diagram of an HPGR (see Fig. 2). Here, a force vector is shown which acts over the IP-Zone and the IS-zone. Only the energy components observed in the IP-zone were considered (they should be the most relevant fractions of the energy consumed).

The compressive force can be estimated by the product of the operating pressure Rp, and the projected area of application, as shown in Eq. (19).

$$F = R_p \frac{D}{2} L \quad (19)$$

The interaction of the clogged material between the rolls and the applied forces generates a reaction torque which is related to the power needed to drive the rolls. The reaction torque (τ) per roll is described by Eq. (20). As observed in the equation, the existence of an angle within the inter particle compression zone is required. This angle corresponds to half of interparticle compression angle, α_{IP} (Klymowsky et al., 2006).

$$\tau = F sin\left(\frac{\alpha_{IP}}{2}\right)\frac{D}{2} \quad (20)$$

The specific energy consumed by the torque in the entire interparticle region, Eq. (21), is obtained by the quotient between the rotational power of the rollers (P_r, Eq. (22)) and the total treatment capacity. Other expressions that use Roll Radial Velocities, and potential volumetric flowrate, could also be used (Rashidi et al., 2017).

$$E = \frac{P_r}{G_{S,i}} \quad (21)$$

$$P_r = 4\tau\frac{U}{D} \quad (22)$$

In order to evaluate the total energy for control applications, the sum of the energy consumed by compression of each block E_c [kWh/kg] (Eq. (23)) and E was carried out (E'). For modelling purposes, only E was considered in Eq. (18). Since different densities and treatment capacities can be evaluated in each section, the compression power was

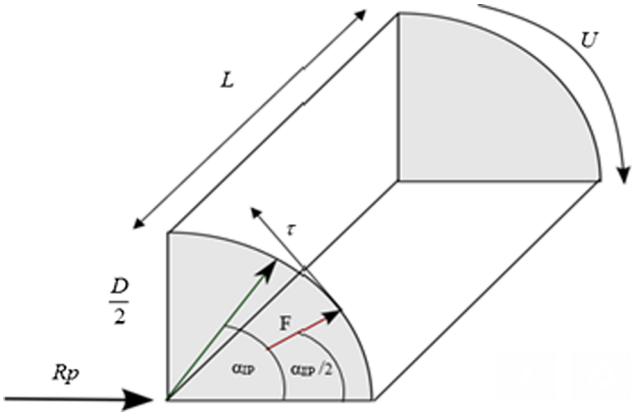

Fig. 2. Free-body diagram of an HPGR roller.

calculated over the sum of the contribution of each *i*-section (Eq. (23)).

$$E_c = \sum_{i=1}^{n} R_p \frac{G_{S,i}}{3.6\rho_{i,cm} G_{S,i+1}} \tag{23}$$

By combining the previous equations (Eqs. (19)–(23)) it is obtained an expression that is non-linear in function of the peripheral velocity, pressure, and other operational parameters, such as the interparticle compression zone. Given this non-linearity and complex dependence of the total used energy, minimization of total energy used should be possible by combining, in specific optimal conditions, the independent variables of the equation system.

The expression given in Eq. (18) possesses different parameters that need to be obtained. Operational parameters and fixed variables, such as O_n, and rolls diameter, among others, are reported in Table 1. Kinetic parameters were determined using the percent passing percentage experimental information reported by Torres and Cassali (2009). In the mentioned work, static HPGR information is reported and modeled for two ores lithologies (Andesitic and Porphyritic) and two manufacturers. Specifically, the open circuit test result with porphyric copper ore at operating conditions of $U = 0.67$ [m/s] and pressures of 41, 61, and 76 [bar] were employed in the present work. Since the experimental information is reported as a static operational condition, the steady-state mode of the model described in Eq. (18) (i.e. the derivative term equal to 0) was used in order to obtain the corresponding parameters.

One of the main considerations to determinate the kinetic parameters was the use of the SP-Zone product as the feed to Eq. (18) (i.e. estimation of $G_{s,0}$ and $P_{j,0}$). Therefore, the feed reported in the work of Torres and Cassali (2009) was previously treated before being considered as input to the IP-Zone. The parameters $k_{0,l}$ and $\Delta E_{d,l}$ were obtained by minimization of the difference between the reported and modeled results, with a restriction that the parameters should be non-negative. Similar to chemical reaction kinetics, a parameter k was first evaluated at each specific power consumption before expressing it in a pre-exponential and in an exponential term. Of the different methodologies used to obtain the parameter, the one that produced the best results was to perform the minimization by steps. In each step, the difference between the data and modeled results for the biggest granulometric size was minimized (followed by the minimization of the next smaller size). It was observed that a minimization of every equation at the same time tended to produce considerable errors for the medium-size granulometric components. Furthermore, once a parameter reached a value of 0, the following parameters where kept equal to 0 (i.e. the smallest granulometric components were not further grinded). Once the parameters were obtained (result section), the pre-exponential terms, $k_{0,l}$, and the exponential term $\Delta E_{d,l}$ were obtained by regression (given by the difference in the pressure used in the HPGR).

3. HPGR model predictive control and integration

Information about MPC is out of the scope of the present work and is broadly covered in the literature. Only the most relevant considerations of the MPC methodologies are mentioned. The classical MPC model is presented in Eq. (24). Λ and Γ are weights vectors that represent the importance of each manipulated and controlled variable; S is a setpoint vector; $y(i+1)$ are the predicted values of the controlled variables up to the prediction horizon (P); $\Delta u(i)$ is a vector of the manipulated variables estimated movements; M is the control horizon; the subindexes *max* and *min* are the maximum and minimum values of the referenced variable, respectively.

$$\begin{aligned} &\sum_{i=0}^{P} [[\Gamma \cdot (y(i+1) - S)]^2 - [\Lambda \cdot \Delta u(i)]^2] \\ &\Delta u = 0, \quad if \quad i \geq M \\ \min_{\Delta u} \quad &\Delta u_{min} \leq \Delta u(i) \leq \Delta u_{max} \\ &u_{min} \leq u(i) \leq u_{max} \\ &y_{min} \leq y(i+1) \leq y_{max} \end{aligned} \tag{24}$$

The optimum obtained in the previous expression will be the most suitable trajectory in the given horizon in such a way that the difference between the system dynamic and the setpoint is minimum. The control variables were selected to represent the HPGR performance and energy consumed. The specific variables that could be used were first screened by considering their static or dynamic behavior. Then, a selection was made by considering the possible data that could be measured in the operational unit, as reported in the work of Daniel and Morrell (2004). The pre-selected variables were the roll speed, bulk compacted density, feed size distribution, working gap, product size distribution, working pressure, power, product size distribution, specific energy, and measured throughput (variables such as sample mass and roll diameter are not considered by its fixed or irrelevant value). Among these variables, the total specific energy (É) and the product size distribution (P_{80}) were chosen as the main controlled variables. Among the manipulated variables, the roll speed and working pressure were selected. The working gap is an indirect manipulated variable since it is normally set by the pressure involved in the hydro-pneumatic system and the initial O_n (Rashidi et al., 2017); therefore this variable was not considered. The roll speed was chosen since, as mentioned in references (Lim et al., 1997), this variable "could be utilized as a major parameter for adjusting the HPGR performance".

A noise of 10% on each particle size mass fraction was incorporated to evaluate controller performance. This was done by ensuring that the total mass fraction always summed up to 1. Before using the preselected variables in the control process, these variables were standardized (Eq. (25); x is the variable to be standardized while the subindexes *diml*, *dim*, *max*, and *min* are used as the dimensionless, with dimension, maximum, and minimum values, respectively).

$$x_{diml} = \frac{x_{dim} - x_{min}}{x_{max} - x_{min}} \tag{25}$$

Table 2 shows the maximum and minimum values used for standardization. The maximum and minimum values were obtained from typical industrial limiting values [6] or from natural restrictions (lower bound of 0). Three sets of tuning parameters were evaluated in order to analyze the effect of the tuning in the control performance. Common parameters for the three sets the P, M, ΔU_{max}, ΔU_{min}, and $\Delta Time$ were 10, 10, 0.003, 0, 0.003, respectively. As solver, the ODE Bogacki-Shampine was used in each case. Weight parameters used are shown in Table 3. As will be seen in the result section, the most satisfactory parameters correspond to those in which the applied pressure, R_p, is less restricted to be used as manipulated variable (smaller Λ; Case II).

The previous equations and control strategy were implemented in Matlab R2010a. Specifically, Simulink was used as main platform where each section (SP-Zone and IP-Zone) was modeled in separated m-files. The Matlab toolbox nlcmpc was used for the controller implementation in which step-response model were employed for HPGR dynamic representation.

4. Results

Model Performance: Table 4 shows the parameters obtained in

Table 1
Parameters for steady state representation.

Variable	Value
On (Operational Gap)	0.024 [m]
U (Peripheral Velocity)	0.67 [m/s]
D (Rolls Diameter)	0.8 [m]
L (Rolls width)	0.25 [M]
β1 (breakage distribution parameter)	0.20
β2 (breackage distribution parameter)	0.20
β3 (breackage distribution parameter)	3.51
ρs (Dry Solid Density [kg/m^3])	2740
ρa (Feed Apparent Density [kg/m^3])	1620

Table 2
Limiting values used for manipulated and controlled variable standardization.

Type of Variable	Variable	Maximum value	Minimum value
MANIPULATED	U [m/s]	1.21	0.67
	R_p [bar]	120	41
CONTROLLED	P_{80} [%]	22	0
	W' [kWh/ton]	27	0

Table 3
Tuning parameters.

Parameter	Case I	Case II	Case III
Λ_U	1	1	0.5
Λ_{Rp}	1	0.5	1
$\Gamma_{E'}$	1	1	1
Γ_{P80}	0.6	0.6	0.6

function of the granulometric size. The second to fourth columns show the kinetic parameter in function of the specific power consumption (1.44, 2.03, and 2.40 kWh/t, respectively). The fifth and sixth column shows the $k_{0,l}$ and $E_{d,l}$ obtained. Furthermore, Table 4 includes different error assessing indexes in order to evaluate the agreement between the modeled and reported information (Mean Square Error, MSE; Root Mean Square Error, RMSE; and Index of Agreement, IA, Eq. (26) in which P_i represent the predicted values, O_i the observed values and $\bar{O}$ the average of the observed values, Willmott et al., 2012). As observed in the table, agreement between the modeled information and the reported data (Torres and Cassali, 2009) is in the order of 99% on each case (IA index), which describes a good performance of the modeled system. Furthermore, by comparing the modeled results with other works (Torres and Cassali, 2009), it can be seen that the MSE obtained by our models is improved. They reported an average of 2.66 with a specific value for the experimental conditions of 2.88; our model obtained a MSE of 1.54 for the same experimental condition (i.e. manufacturer M1 and porphyric copper ore at 41 bar and 0.67 m/s of peripheral velocity).

$$IA = 1 - \frac{\sum_{1=1}^{n} (P_i - O_i)^2}{\sum_{i=1}^{n} (|P_i - \bar{O}| + |O_i - \bar{O}|)^2} \quad (26)$$

MPC Performance: Fig. 3 shows the MPC system response for the three cases described in Table 3. The analysis was performed by modifying the setpoints in the controlled variables. The $\acute{E}$ was changed from 0.6 to 0.75 to 0.45 to 0.7 (in dimensionless variables units) at times of 15, 50, and 75 s, respectively. The P_{80} was modified from 0.8 to 0.6 to 0.45 at 15 and 75 s, respectively. At first glance, there is almost no difference in the control behavior of the MPC when the tuning parameter changes. The behavior shows fast responses and that the manipulated variables follow with no major problem the requirement set over them. Oscillation was observed on each case, but no correlation with the implemented noise was observed.

Since a manipulated variable is the total energy consumed by the system, its value can be manipulated up to a certain minimum and maximum limit. After these limits, it would not be possible to control the product granulometry (lower bound) or holds (not predicted by the model) could be observed. The lower bound implies that if the energy imposed over the system is too low, it would be not sufficient to produce the grinding requirement. In this work, regions in which both controlled variables that could be modified without inconvenient results were considered. The minimum conditions for each controlled variable can be implemented in the MPC formulation; nevertheless, they would have to be studied case by case for industrial application.

Fig. 4 shows a closeup of Fig. 3 between the seconds 48.7 and 49 of simulation. The E' was selected as variable to evaluate the performance of the three cases. The case II tuning, which implies a lower restriction to use the pressure as manipulated variable, produced the smallest amplitude of the oscillation observed (with an average of 0.00086 in dimensionless units; Case I showed a value of 0.00110 and Case III showed a value of 0.00100). Nevertheless, the number of oscillations per cycle (per second) was observed to be higher for Case II (7.75 oscillations/second; 7, approximately for Case I and Case III).

By considering set point deviations, it can be established that the tuning Case II overperforms the other tunings; however, in terms of stability (indicated by the number of oscillations) the other cases perform better. This result shows that a tradeoff between number of oscillations and approximation to the setpoints must be performed for the current MPC proposed. Independent of these results, the work establishes a need to perform a correct tuning for each possible industrial application in order to obtain a desirable performance (i.e. product granulometric distribution at a given energy consumed) with a stable controller.

5. Conclusion

A multivariable controller was designed and implemented in a HPGR dynamic model. The model was created by considering variable volumes resulting from dividing the pre-crushing zone in horizontals blocks. The model parameters were obtained by minimization using the information of the steady state reported data. The model and the controller were developed in Matlab (Simulink). A MIMO controller was created considering energy correlated variables, such as the peripheral velocity and operational pressure, and energy variables, such as the total energy consumed. As result it was observed that the selections of variables are suitable manipulated variables to control the total energy

Table 4
Kinetic Parameters and Error Assessing Indexes of the Model.

Size [mm]	K (1.44 kWh/t)	K (2.03 kWh/t)	K (2.40 kWh/t)	K_0 [1/s]	$\Delta E_{d,l}$ [kWh/t]
31.50	38.43	65.00	150.00	769.85	4.43
22.40	14.98	22.95	25.91	60.43	2.00
16.00	15.56	24.43	20.64	39.12	1.27
11.20	17.79	23.85	22.87	36.73	1.02
8.00	15.91	20.44	22.30	37.17	1.22
5.60	4.71	7.35	8.25	19.77	2.06
2.80	0	0	0	0	–
1.00	0	0	0	0	–
0.50	0	0	0	0	–
0.32	0	0	0	0	–
0.20	0	0	0	0	–
0.13	0	0	0	0	–
MSE/RMSE/IA	1.54/ 1.24/0.99	0.46/ 0.68/0.99	0.1024/ 0.32/0.99	1.59/1.26 (1.44 kWh/t)/0.99	

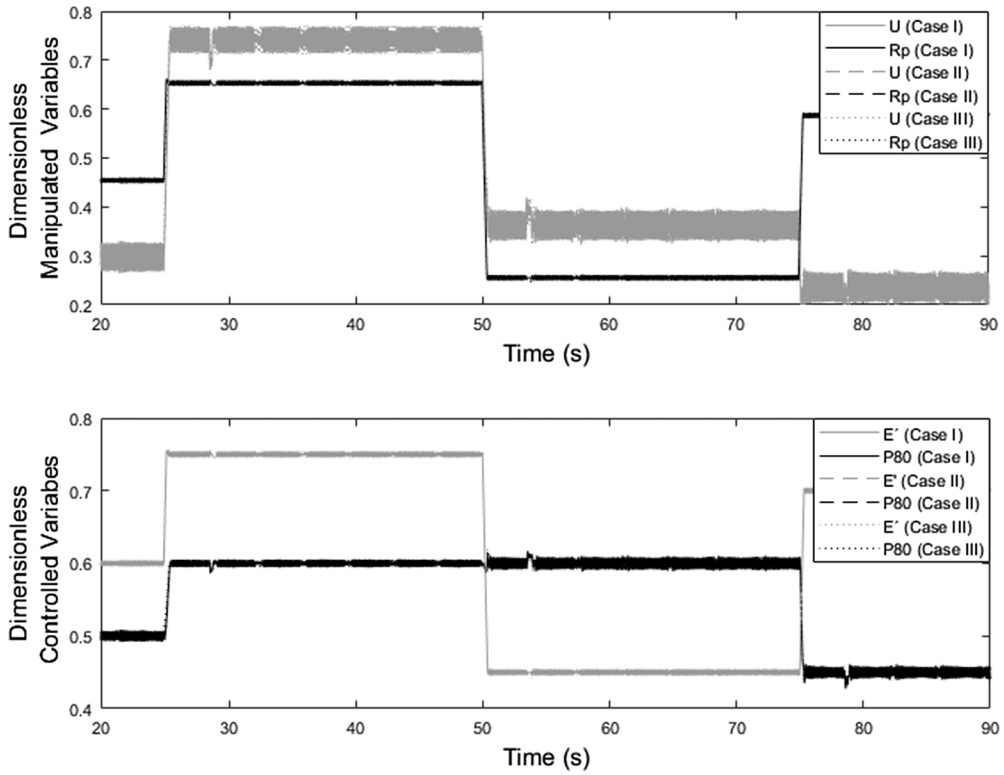

Fig. 3. MPC results when performing set point variation.

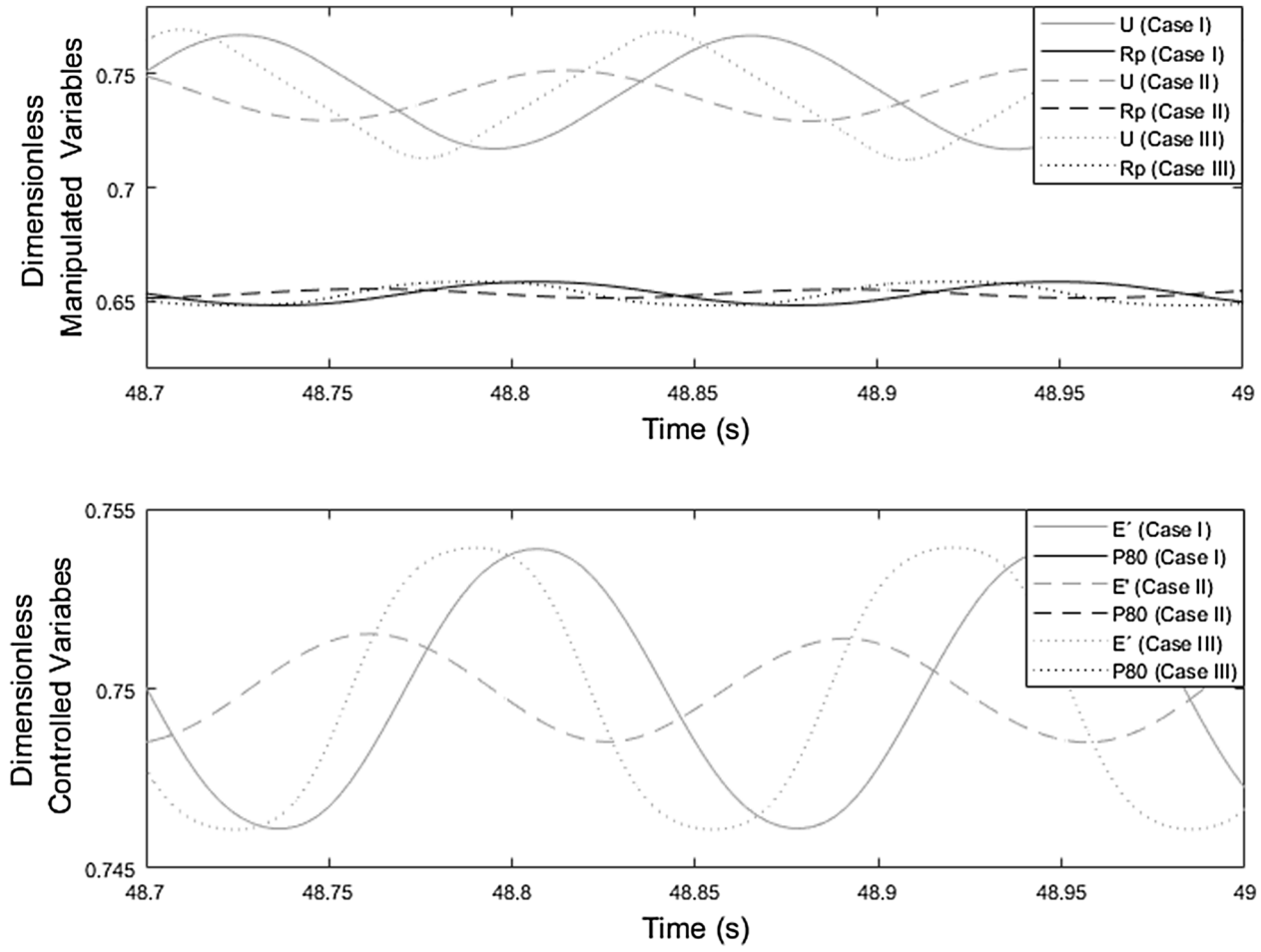

Fig. 4. Relative Oscillation and amplitudes behavior in the control process.

consumption and the granulometric distribution (reported as P_{80}). The tuning of the controller was developed considering a set of parameters, in which the weights were evaluated for the manipulated variables. As observed in the result, the minimal weight in the pressure manipulated coefficient allows lower deviations with respect to the set point to be obtained (measured as amplitude of the oscillation; 0.00086 in dimensionless units). The present work supports the incorporation of an MPC controller in grinding operational units. Nevertheless, a considerable tuning study would be required for the application to specific industrial applications. It is likely that the control strategy could improve operational costs by saving energy; this needs to be confirmed by carrying out tests at plant scale.

Acknowledgment

The authors acknowledge the help from the different international institutions that have given support to the researchers and institutions involved in the project. Specially we acknowledge the Universidad de las Fuerzas Armadas, Ecuador; The Universidad Central de Chile, Chile; The Science Foundation Ireland, Ireland; and the European Regional Development Fund.

References

Austin, L.G., Klimpel, R.R., Luckie, P.T., 1984. Process engineering of size reduction: Ball milling. Society of Mining Engineering of the AIME, New York.
Barani, K., Balochi, H., 2016a. A comparative study on the effect of using conventional and high pressure grinding rolls crushing on the ball mill grinding kinetics of an iron ore. Physicochem. Probl. Mi. 52 (2), 920–931.
Barani, K., Balochi, H., 2016b. First-order and second-order breakage rate of coarse particles in ball mill grinding. Physicochem. Probl. Mi. 52 (1), 268–278.
Barrios, G.K.P., Tavares, L.M., 2016. A preliminary model of high pressure roll grinding using the discrete element method and multi-body dynamics coupling. Int. J. Miner. Process. 156 (10), 32–42.
Bouché, C., Brandt, C., Broussaud, A., van Wayne, D., 2005. Advanced control of gold ore grinding plants in South Africa. Miner. Eng. 18 (8), 866–876.
Cao, J.Y., Cao, B.G., 2006. Design of fractional order controller based on particle swarm optimization. Int. J. Control Autom. 4 (6), 775–781.
Chapman, N.A., Shackleton, N.J., Maysiak, V., O'Connor, C.T., 2013. Comparative study of the use of HPGR and conventional wet and dry grinding methods on the flotation of base metal sulphides and PGMs. J. S. Afr. I. Min. Metall. 113, 407–413.
Conradie, A.V.E., Aldrich, C., 2001. Neurocontrol of a ball mill grinding circuit using evolutionary reinforcement learning. Miner. Eng. 14 (10), 1277–1294.
Daniel, M.J., Morrell, S., 2004. HPGR model verification and Scale-up. Miner. Eng. 17 (11–12), 1149–1161.
Hinde, A.L., Kalala, J.T., 2009. The application of a simplified approach to modelling tumbling mills, stirred media mills and HPGŔs. Miner. Eng. 22 (7–8), 633–641.
Jankovic, A., Valery, W., Sönmez, B., Valle, R. (2013). Effect of classification efficiency on HPGR and ball mill circuit capacity. In: XXX Convención Internacional de Minería, Acapulco, Gro., México, Octubre 16-19.
Jeswiet, J., Szekeres, A., 2016. Energy consumption in mining comminution. Procedia CIRP 48, 140–145.
Lim, W.I.L., Campbell, J.J., Tondo, L.A., 1997. The effect of rolls speed and rolls surface pattern on high pressure grinding rolls performance. Miner. Eng. 10 (4), 401–419.
Monov, V., Sokolov, B., Stoenchev, S., 2012. Grinding in ball mills: modeling and process control. Cybernet. Information Technol. 12 (2), 51–68.
Morrell, S., Shi, F., Tondo, L.A. (1997). Modelling and Scale-up of High Pressure Grinding Rolls. In: Proceedings of the XX International Mineral Processing Congress (IMPC), Aachen, Germany, Septembre 1997.
Morley, C., 2006. High–pressure grinding rolls – a technology review. SME Inc., pp. 15–39.
Palm, N.A., Shackleton, N.J., Malysiak, V., O'Connor, C.T., 2010. The effect of using different comminution procedures on the flotation of sphalerite. Miner. Eng. 23 (11–13), 1053–1057.
Ramasamy, M., Narayanan, S.S., Rao, Ch.D.P., 2005. Control of ball mill grinding circuit using model predictive control scheme. J. Process Control 15 (3), 273–283.
Rosario, P.P., 2017. Technical and economic assessment of non-conventional HPGR circuit. Miner. Eng. 103–104, 102–111.
Salazar, J.L., Valdés-González, H., Vyhmeister, E., Cubillos, F., 2014. Model predictive control of semiautogenous mills (SAG). Miner. Eng. 64, 92–96.
Schönert, K., 1985. Sizing of high pressure twin roll mills. Zement Kalk Gips 12, 728–730.
Schönert, K.A., 1988. First survey of grinding with high-compression roll mills. Int. J. Miner. Process. 22, 401–412.
Torres, M., Cassali, A., 2009. A novel approach for the modelling of high-pressure grinding rolls. Miner. Eng. 22 (13), 1137–1146.
Tromans, D., 2008. Mineral comminution: Energy efficiency considerations. Miner. Eng. 21 (8), 613–620.
Whiten, W.J., 1973. The simulation of crushing plants. Application of computer methods in the mineral industry. APCOM10. African Inst. Min. Metall., Johannesburg 317–323.
Fuerstenau, D.W., Gutsche, O., Kapur, P.C., 1996. Confined particle bed comminution under compressive loads. Int. J. Miner. Process. 44–45, 521–537.
Rashidi, S., Rajamani, R.K., Fuerstenau, D.W., 2017. A review of the modeling of high pressure grinding rolls. KONA Powder Part. J. 34, 125–140.
Fuerstenau, D.W., Shukla, A., Kapur, P.C., 1991. Energy consumption and product size distribution in choke-fed, high compression roll mills. Int. J. Miner. Process. 32, 59–79.
Klymowsky, R., Patzelt, N., Knecht, J., Burchardt, E. (2006). An overview of HPGR technology. In: International Conference on Autogenous and Semiautogenous Grinding Technology, pp. 11–26.
Altun, O., Benzer, H., Dundar, H., Aydogan, N.A., 2011. Comparison of open and closed circuit HPGR application on dry grinding circuit performance. Miner. Eng. 24, 267–275.
Willmott, C., Robeson, S.M., Matsuura, K., 2012. A refined index of model performance. Int. J. Climatol. 32, 2088–2094.